CONTROL OF FLAP VORTICES

David Greenblatt
Flow Physics & Control Branch, NASA Langley Research Center, Hampton, VA 23681

ABSTRACT

A wind tunnel investigation was carried out on a semi-span wing model to assess the feasibility of controlling vortices emanating from outboard flaps and tip-flaps by actively varying the degree of boundary layer separation. Separation was varied by means of perturbations produced from segmented zero-efflux oscillatory blowing slots, while estimates of span loadings and vortex sheet strengths were obtained by integrating wing surface pressures. These estimates were used as input to inviscid rollup relations as a means of predicting changes to the vortex characteristics resulting from the perturbations. Surveys of flow in the wake of the outboard and tip-flaps were made using a seven-hole probe, from which the vortex characteristics were directly deduced. Varying the degree of separation had a marked effect on vortex location, strength, tangential velocity, axial velocity and size for both outboard and tip-flaps. Qualitative changes in vortex characteristics were well predicted by the inviscid rollup relations, while the failure to account for viscosity was presumed to be the main reason for observed discrepancies. Introducing perturbations near the outboard flap-edges or on the tip-flap exerted significant control over vortices while producing negligible lift excursions.

1. INTRODUCTION

The prediction and control of vortices trailing in the wakes of wings and rotors is a problem of significant technological importance. Large aircraft on approach for landing generate powerful trailing vortices that pose a severe and potentially catastrophic aerodynamic hazard to following aircraft (e.g. Spalart [1] and Rossow [2]). Several accidents have been attributed to these vortices, also referred to loosely as wake turbulence, in recent decades. Regulatory rules that govern the minimum separation distances between aircraft lead to delays that are longer than those dictated by other factors, and this exacerbates airport congestion [3].

Viable wake vortex alleviation has been attempted using two main approaches: time-invariant methods and time-dependent methods. Time-invariant methods rely on modifying the span loading to establish two or more pairs of opposite-signed counter-rotating vortices, where naturally arising instabilities bring about their linking and mutual destruction (e.g. Cliffone & Orloff [4] and Ortega *et al*. [5]). Time-dependent methods that actively force the breakup of vortices are realized, for example, by pitching the aircraft (Chevalier [6]) or differentially deflecting inboard and outboard control surfaces (e.g. Crow and Bate [7] and Crouch *et al*. [8]). Despite their inherent appeal, active methods must address issues such as "ride quality, dynamic-load effects on the structure, and the ability to maintain control authority during operation" (Crouch [9]).

To achieve the relatively low speeds required for take-off and landing, modern airliners deploy a complex system of flaps, generally termed a high-lift system (e.g. Rudolph [10] and van Dam [11]). The vortices emanating from the flap-edges dominate the ensuing wake structure (e.g. Bellastrada *et al*. [12]), but are susceptible to relatively short wavelength, fast-growing instabilities as well as transient growth mechanisms, which depend strongly on the vortex characteristics (Crouch [13]). High-lift systems, however, are aerodynamically inefficient due to flow separation, particularly on the flaps and in the wing-flap cove region. Nevertheless, separated flows are amenable to active control or manipulation, for example, by means of

periodic excitation (e.g. Greenblatt & Wygnanski [14]). Thus separated flow can be viewed as an "exploitable resource" that is a "by-product" of the high-lift system. In this sense, actively varying the degree of separation brings about variations in the bound circulation (Γ) – hence the vortex sheet strength ($\gamma = d\Gamma/dy$) – and ultimately the wake structure. Furthermore, applying control over different parts of the flap periodically potentially allows time-dependent control of the vortices by so-called "sloshing" of the lift distribution on the flap [7].

An additional unrelated trailing vortex problem is the generation of helicopter noise and vibration that arise from the interaction of rotor blade tip-vortices with succeeding blades as well as the airframe, empennage and tail rotor of the vehicle (Leishman [15]). In particular, blade-vortex interaction (BVI) is responsible for most of the sound pollution caused by helicopters, particularly during low-speed landing approach and maneuvers, and is also a main contributor to ground noise during level flight. Driven by increasingly stringent certification requirements and public acceptance, BVI noise reduction has received considerable attention, with many varied techniques proposed to alleviate the problem.

One approach to the problem involves the reduction in vortex strength while simultaneously increasing vortex core size (e.g. McAlister *et al.* [16] and Lui *et al.* [17]), but invariably result in a degradation of overall rotorcraft performance. A different approach is based on increasing the distance between the vortex and the rotor blade and thereby minimizing the interaction, using active flaps (e.g. Dawson *et al.* [18]), higher harmonic control of blade pitch (e.g. Splettstößer *et al.* [19]), or individual blade control (Jacklin & Nguyen [20]). However, deploying these devices leads to flow separation, which results in increased drag and flow unsteadiness, while higher harmonic and individual blade control inputs can themselves promote and increase in vibrations.

2. OBJECTIVES & SCOPE

A pilot study was undertaken at NASA Langley Research Center to determine the feasibility of controlling trailing vortices, in the open-loop sense, by actively varying the degree of flow separation on deflected flaps. This was achieved using a semi-span model where separation was enforced locally by means of two independent flaps. Segmented zero-mass-flux oscillatory blowing was then used to vary the degree of flow separation, thereby controlling the trailing vortices. The model, measurements and data reduction techniques are described in section 3 and theoretical rollup relations are developed in section 4. A discussion of the data and a comparison with the inviscid rollup relations is presented in section 5.
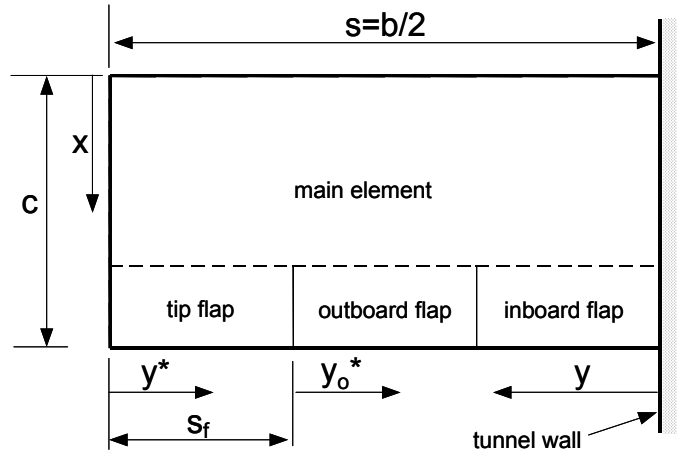
Fig. 1. Schematic showing the semi-span model coordinate systems and definitions.

3. EXPERIMENTAL SETUP

Experiments were performed on a rectangular planform semi-span NACA 0015 port-side model wing of aspect ratio $AR=4$ (semi-span $s=609.6$mm, chord $c=304.8$mm) cantilevered off the wall of a low-speed wind tunnel. The model comprised a main element and three simple flaps (inboard, outboard, and tip) of equal span ($s_f=s/3$), with the hingeline at the 70% chord (fig. 1). The coordinate system used in this paper is defined in the figure. Two specific configurations were considered, namely outboard-flap deflection: $(\delta_i,\delta_o,\delta_t)=(0°,20°,0°)$ and tip-flap deflection: $(\delta_i,\delta_o,\delta_t)=(0°,0°,20°)$. Each flap was equipped with a zero-efflux blowing slot at its shoulder of width $h=0.76$mm. Zero mass-flux perturbations through the slots (fig. 2a) were produced via voice-coil type actuators (J. Kiedaisch, H. Nagib & Associates, IIT) that generated pressure fluctuations within slot sub-plenums. Perturbations were calibrated using a hot wire anemometer and characterized by a dimensionless frequency $F^+=fL_f/U_\infty$ and a momentum coefficient $C_\mu=h/c(u_j/U_\infty)^2$, where $L_f=0.3c$ and u_j is the peak slot velocity. F^+ and C_μ were selected on the basis of previously established criteria [14]. Only slots corresponding to the deflected flaps (outboard and tip) were employed for this investigation. In addition, the inboard and outboard halves of the outboard flap were operated independently (fig. 2a). All data were acquired at Reynolds numbers ($Re=U_\infty c/\nu$) of 500,000 and 1,000,000, where a leading-edge trip rendered the aerodynamic coefficients effectively Re independent.
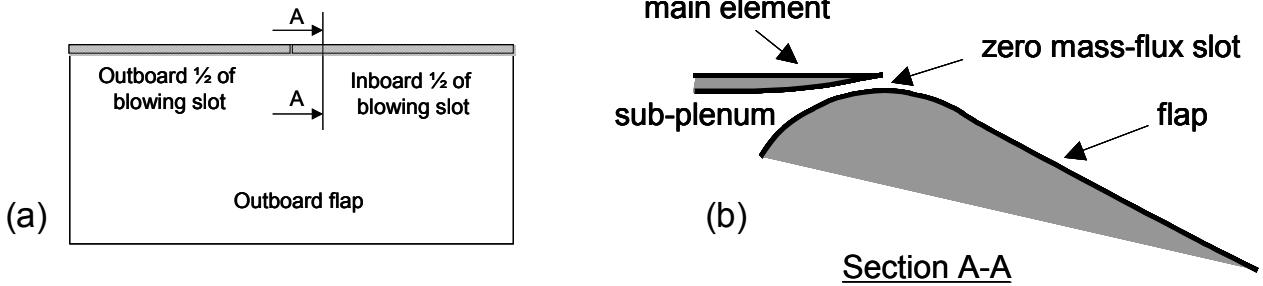
Fig. 2a. Schematic of the midspan flap, showing the inboard and outboard slot locations.

Fig. 2b. Close-up section of the flap-slot region illustrating the technique used to introduce zero mass-flux perturbations.

The model was equipped with 165 static pressure ports arranged in a perpendicular spanwise and chordwise grid. Integration of these surface pressures allowed estimation of span loading and vortex sheet strength, which were used to calculate vortex characteristics (see section 4 below). The model was also equipped with nine dynamic pressure transducers on the wing upper surface.

Wing static pressures were measured using an electronic pressure scanner and unsteady pressures were measured by means of piezoresistive pressure transducers. A 1.6 mm diameter seven-hole probe, with accuracy better than 1% on the velocity magnitude and 0.5 degrees on the flow angles, was used to make wake measurements of (U,V,W), as a function of (y,z), at $x/c=2$.

Streamwise vorticity was calculated according to:

$$\omega_x = \partial W / \partial y - \partial V / \partial z \tag{1}$$

using central differences. Vortex strength in the wake and the vortex centroid were determined by means of the standard definitions:

$$\Gamma_w = \int \omega_x dA \tag{2}$$

and

$$(\bar{y}_w, \bar{z}_w) = \frac{1}{\Gamma_w} \int (y,z)\omega_x dA \qquad (3)$$

The tangential velocity (V_θ) and radial coordinate (r) were determined from the in-plane velocity components (V, W) and (y, z) coordinates relative to the vortex centroid respectively, and $V_x = U$. This allowed direct determination of the peak tangential velocity and the corresponding radius (r_1). Experimental scatter precluded an accurate estimate of r_2 (radius at which the tangential velocity blends with the point vortex field [1]).

4. WAKE-STRUCTURE PREDICTIONS USING INVISCID ROLLUP RELATIONS

Predicting the effect of separated flow manipulation on flap vortex characteristics was achieved using the method of Betz, in the form developed by Donaldson *et al*. [21]. Betz's method does not explicitly treat the rollup mechanism, but rather employs three conservation relations between the span-loading $\Gamma(y)$ and the rolling-up vortex $\Gamma'(r)$. Betz employed the conservation of vorticity (see eqn. 5 below), and also postulated that the first and second moments of vorticity are conserved (see eqns. 4 and 6 below). Despite the relative simplicity of the method, Donaldson [22] showed that it predicts flap vortex details that are in surprisingly good agreement with aircraft-wake wing-tip vortices.

Based on these successful predictions, Donaldson *et al*. [21] extended the method to include flapped wings and once again demonstrated excellent agreement with experimental data. Implementation of the method to this vortex control problem presented a difficulty due to the dearth of theoretical or computational methods capable of accurately predicting the effects of zero-efflux perturbations. In order to circumvent this problem, modeling input resulting from separation manipulation, namely $\Gamma(y)$ and $\gamma(y)$, were determined empirically by integrating wing surface pressures (see section 2).

Implementing the Donaldson-Betz method for the present investigation is described with respect to fig. 3. The upper part of the figure shows the lift distributions that result from a deflection of the outboard flap ($\delta_o = 20°$), without separation control (baseline case) and with separation control applied on the inboard half (see fig. 2b) of the flap (controlled case). The lines are polynomial least squares curves, fitted to data points in the vicinity of the flap-edges. The lower part of the figure shows the rolled-up vortices in the so-called Trefftz plane, which is defined as the plane behind the wing that is perpendicular to the direction of, and moves with, the free-stream. For relatively complex wing-load distributions, such as that shown in fig. 3, Donaldson *et al*. [21] showed that circulation becomes multi-valued during the roll-up calculation and thus a single vortex rollup is not physically possible. They assumed that the vorticity shed between adjacent local $|d\Gamma/dy|$ minima rolls-up into individual vortices and that the local shed vorticity peak between the adjacent minima ($|d\Gamma/dy|_m$), located at $y = y_m$, progresses into the center of the vortex. Using these criteria, the method predicts three roll-up vortices in the Trefftz plane (fig. 3), which is consistent with observations, at least in the near field considered here ($x/c \leq 2$). Note that the relatively low pressures at the wing-tip result from the wing-tip vortex that is partially rolled-up on the upper surface. Without further approximation, this precludes the application of rollup relations to the tip vortex.
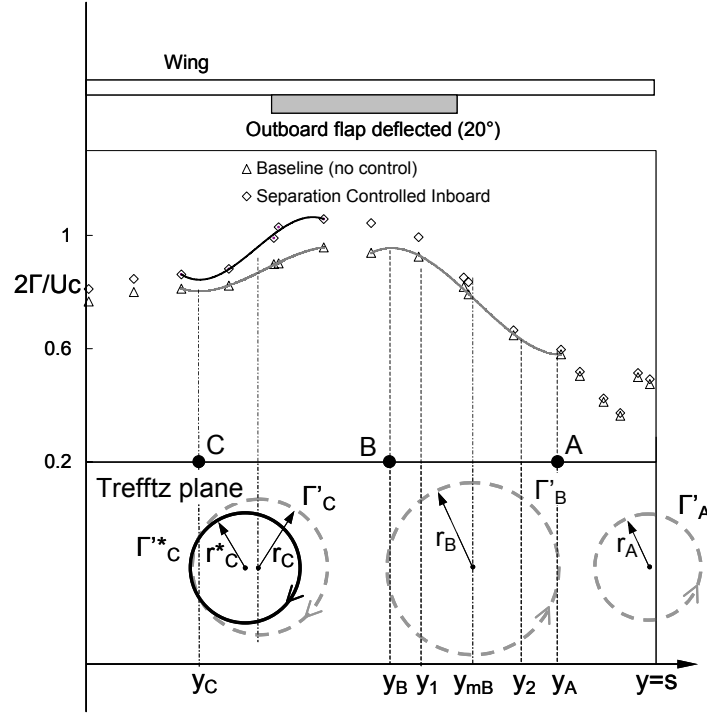
Fig. 3. Experimental data with a schematic illustrating the Donaldson-Betz vortex rollup method between the span-loading and the Trefftz plane.

Applying the method to the outboard flap vortex (B), the vorticity between adjacent $|d\Gamma/dy|$ minima y_A and y_B rolls-up into a vortex located at the centroid defined by:

$$\bar{y}_B \int_{y_A}^{y_B} \frac{d\Gamma(y)}{dy} dy = \int_{y_A}^{y_B} y \frac{d\Gamma(y)}{dy} dy \tag{4}$$

In addition, the remaining invariants described above can be written as:

$$-\int_{y_1}^{y_2} \frac{d\Gamma(y)}{dy} dy = \int_0^{r_B} \frac{d\Gamma'_B(r)}{dr} dr \tag{5}$$

and

$$-\int_{y_1}^{y_2} (y - \bar{y}_{12})^2 \frac{d\Gamma(y)}{dy} dy = \int_0^{r_B} r^2 \frac{d\Gamma'_B(r)}{dr} dr \tag{6}$$

If we choose y_1 and y_2 to be equidistant from the centroid of shed vorticity, from eqn 5 we can write

$$\Gamma'_B = \int_{y_A}^{y_B} \frac{d\Gamma}{dy} dy = \Gamma(y_A) - \Gamma(y_B), \tag{7}$$

where the centroid, from eqn. 4, is located at

$$\bar{y}_B = \frac{1}{\Gamma'_B} \int_{y_A}^{y_B} y \frac{d\Gamma}{dy} dy. \tag{8}$$

and the radius at which the tangential velocity blends with the point vortex field [1], from eqn. 6, is:

$$r_B = \frac{y_B - y_A}{2} \tag{9}$$

5

Finally, using the equation for an inviscid vortex, and a relation similar to that of equation (6), the tangential velocity at the center of the vortex is:

$$V_{\theta B}(0) = -\frac{1}{\pi}\left(\frac{d\Gamma}{dy}\right)_{y=y_{mB}} \tag{10}$$

The relations expressed in equations (4) to (6) provide four basic characteristics of the rolled-up vortex.

The above rollup relations can also be applied to the inboard vortex (C), where both baseline and controlled scenarios are shown for purposes of illustration (asterisks indicate active manipulation of separation). Simplifying assumptions associated with the above method, e.g. Moore & Saffman [23], are well known. Nevertheless, when applying the method to a flow control problem, the limitations become less important when comparing *changes* between baseline (uncontrolled) and controlled states, for example $\Delta\bar{y} = \bar{y}^* - \bar{y}$, $V_\theta^*(0)/V_\theta(0)$, Γ'^*/Γ', and $\Delta r_2 = r_2^* - r_2$. Furthermore, given the relative simplicity and rapidity of span-loading measurements versus wake-surveys, the method is particularly useful for ascertaining trends.

5. EXPERIMENTAL DATA & COMPARISON WITH ROLLUP RELATIONS
### 5.1 Outboard Flap Actuation

Separation control is most commonly applied to increase lift on an airfoil or wing. In contrast, when employing a scheme for perturbing vortices it is desirable to maximize vortex control authority while simultaneously minimizing the effect on lift excursions. To illustrate these seemingly contradictory requirements, consider the differences between uncontrolled (baseline) and controlled scenarios at various angles of attack (α) where perturbations are introduced along the entire outboard flap span (figs. 4a and 4b). We see here that the changes to both $\Gamma(=C_l U_\infty c/2)$ and γ are substantial. Thus, we seek to minimize changes to the former while simultaneously maximizing authority over the latter. Consider furthermore the effect of increasing control amplitude (C_μ) on the lift and moment coefficients at $\alpha=8°$ (fig. 5). For separation control on airfoils under similar conditions, in the absence of boundary layer transition and strong curvature effects, typically $\Delta C_L \propto \ln(C_\mu)$. In contrast, lift and moment changes to the wing are not proportional to C_μ.
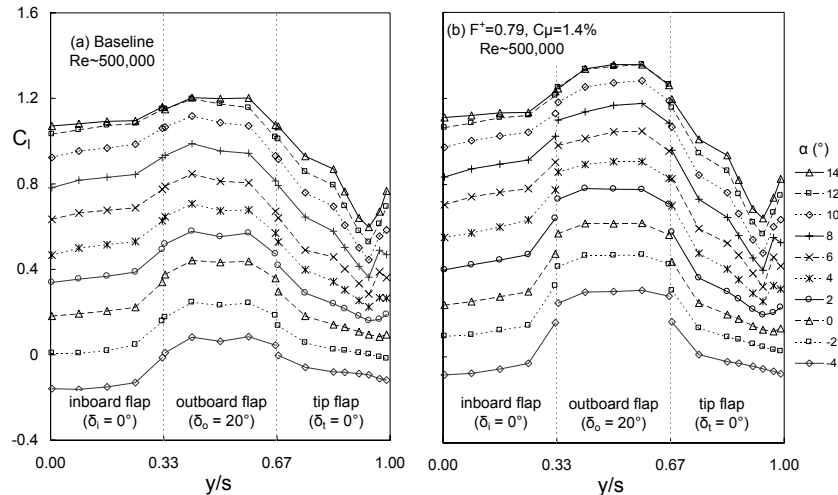
Fig. 4. Span loading generated with and without active perturbations on the outboard flap (a) baseline; (b) controlled.
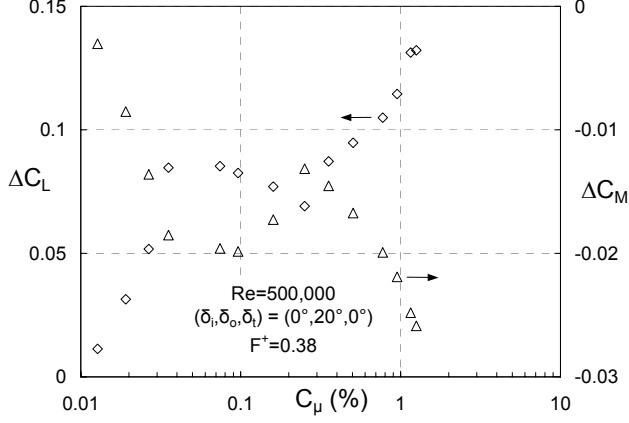
**Fig. 5.** Effect of increasing midspan perturbation amplitude on overall wing lift and moment coefficients ($\alpha=8°$).
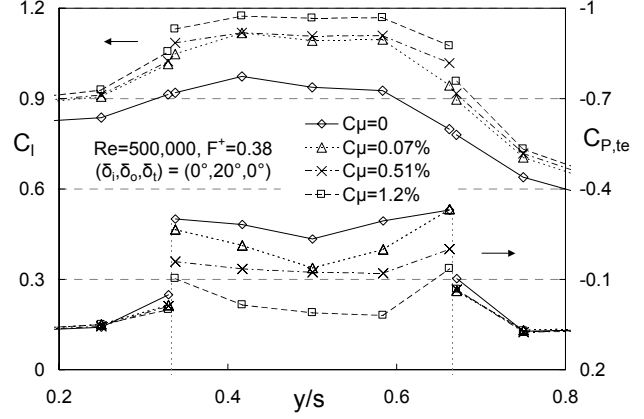
Fig. 6. Spanwise flap trailing-edge pressure recovery for increasing midspan perturbation amplitude ($\alpha=8°$).

More insight into this non-proportionality can be seen from fig. 6, which shows the span-loading and flap trailing-edge pressures for various forcing amplitudes in the vicinity of the flap. At low amplitudes the pressure recovery is mainly evident in the central part of the flap and this is associated with a relatively large increase in lift. Further increases in control amplitude up to $C_\mu \approx 0.2\%$ do not have a marked effect on the pressure recovery and this corresponds to the small changes in aerodynamic coefficients (cf. fig. 5). For $0.25\% \leq C_\mu \leq 0.5\%$, pressure recoveries are evident at the flap-edges, consistent with edge vortices being brought towards the surface, and this is reflected in the renewed changes to the aerodynamic coefficients (fig. 5). Further increases in amplitude bring about greater recovery along the entire flap span, but the effects at the inboard and outboard edges are relatively small.

Perturbations to the flap vortices, calculated by means of the inviscid vortex relations (eqns. 7-10), are shown in figs. 7a-d. As expected, the vortex strength and peak velocity vary in accordance with the loading on the flap (figs. 7b and 7c). Although the ratios of outboard vortex strength and peak tangential velocities are smaller than those associated with the inboard vortex, the corresponding baseline and controlled absolute values are typically twice as large. The rollup relations predict a greater effect on the centroid of the outboard vortex than the inboard vortex (fig. 7a). This is due to the relatively large changes in loading near the outboard edge. However, the centroids do not exhibit the non-proportional behavior because the loading near the flap-edges varies in a different manner to that in the central part of the flap. Almost full authority is exerted over them for $0.01 < C_\mu < 0.5$, corresponding to a relatively small change in lift: $\Delta C_L < 0.05$ (fig. 5). The same is true for the size of the vortex (fig. 7d).

Seven-hole probe measurements of streamwise and in-plane velocity are shown in the wake of the flap at $x/c=2$ for the baseline case (fig. 8a and 8b) and for the controlled case with $F^+=0.38$ and $C_\mu=1\%$ (fig. 8c and 8d). Vortex characteristics were calculated according to eqns. 1-3 and compared with the rollup relations in table 1. In general, the rollup predictions are superior for the outboard vortex. This may be an inherent limitation of the rollup method, which was not validated for counter-rotating vortices [21,24]. Of importance from a practical standpoint is that far greater authority is attainable over the inboard vortex centroid than that predicted by the rollup

7

relations. In fact, the authority is greater than 2% of the semi-span for both inboard and outboard vortices. In contrast to the rollup predictions, measured changes to the strength of both inboard and outboard vortices are similar when each is referenced to its baseline value, i.e. the relative strength of the vortices remains constant for baseline and control. Predictions of the peak velocity ratios are poor, especially for the inboard vortex (see discussion below).
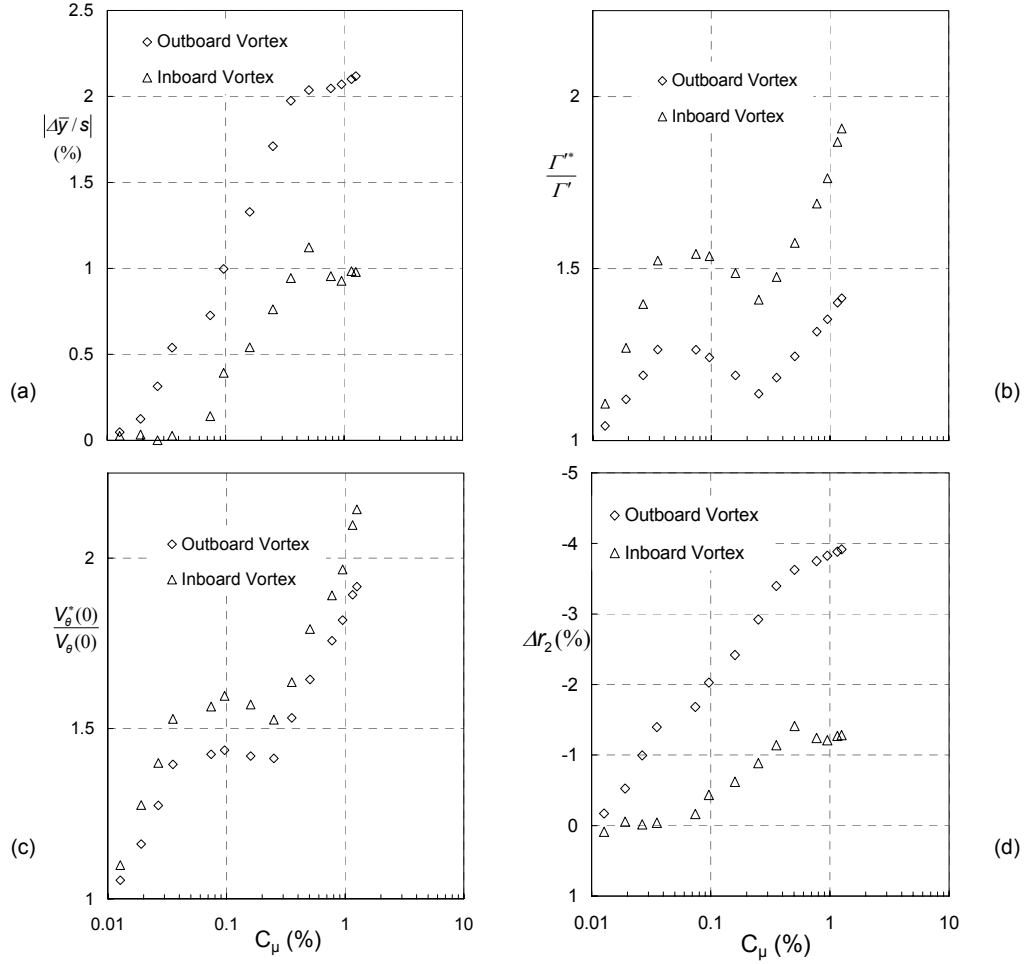
Fig. 7. Donaldson-Betz rollup predictions of vortex characteristics as a function of forcing amplitude corresponding to the data in figs. 5 and 6.

Table 1. Effect of separation control on the midspan flap trailing vortices.

	Outboard Vortex (B)		Inboard Vortex (C)	
	7-hole probe	Donaldson-Betz	7-hole probe	Donaldson-Betz
$\Delta \bar{y} / s$ (%)	-2.32	-2.07	2.62	0.93
Γ'^* / Γ'	1.36	1.35	1.35	1.76
$V_\theta^*(0)/V_\theta(0)$	1.44	1.82	1.08	1.97
r_1^* / r_1	0.49	—	0.57	—
r_2^* / r_2	—	0.74	—	0.90

8
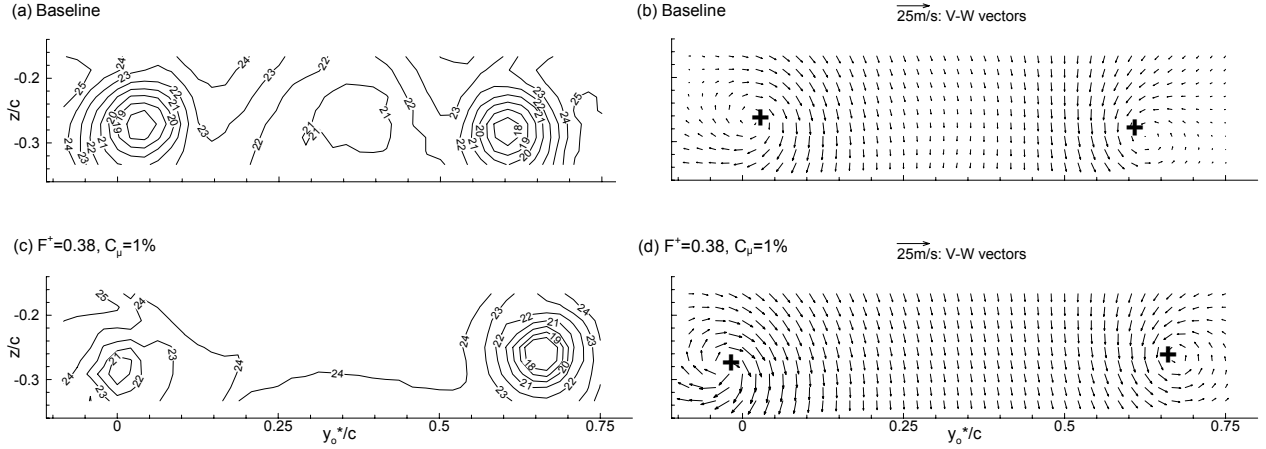
Fig. 8. Seven-hole probe measurements in the wake of the outboard flap at x/c=2 for axial velocity (U or V_x) and in-plane velocity vectors (V-W) with vortex centroids identified: (a,b) baseline; (c,d) control (α=8°).

The discrepancies between the predictions and wake measurements are due to limitations associated with both. The primary limitation of the wake measurement is its relatively close proximity to the wing (x/c=2). Note, however, that further downstream the vortices become more mature (axi-symmetric), but they are also subject to the effects of neighboring vortices and wind tunnel walls. The main limitation of the theoretical method is its neglecting of viscosity. This may be a valid assumption for wings that have fully attached boundary layers. But for flows that have large separated shear layers, such as those over flaps, this assumption is difficult to defend.

The wake flow between the vortices shows a significantly smaller momentum deficit when control is applied and this is consistent with lower drag that is associated with separation control (cf. figs. 8a and 8c). The axial flow in the vicinity of the vortex centerline, however, behaves differently for the inboard and outboard vortices. The inboard vortex centerline velocity decreases slightly while the outboard vortex centerline increases by about $0.3U_\infty$. The reason for the inboard deficit is not known, but the outboard velocity increase can be explained qualitatively using Batchelor's [25] analysis, by considering a streamline which extends from upstream of the wing through the vortex centerline where, by definition, $V_\theta = V_r = 0$. The axial velocity on the centerline can then be written as:

$$\frac{V_{xc}}{U_\infty} = \sqrt{1 + \frac{(p_\infty - p_c) - \rho g \Delta H}{\rho U_\infty^2 / 2}} \tag{11}$$

where the first term in the quotient on the rhs is the pressure drop in the vortex [$\propto (\Gamma'/r_1)^2$] and the second term is a head-drop representing viscous losses. Considering the increased circulation and decreased size associated with the controlled vortex (table 1), it is clear from eqn. 11 that separation control acts to increase the centerline axial velocity. As alluded to above, the viscous losses in an attached boundary layer are significantly less than those in a thicker separated shear layer. Thus control acts to further increase the centerline velocity by reducing the viscous head drop. It is therefore a combination of increased pressure drop and decreased head-drop that are jointly responsible for the higher axial velocities. In addition, Donaldson & Bilanin [24] point out that $V_\theta(0) \propto (V_{xc}/U_\infty)^{1/2}$ which is not taken into account in the rollup relations and may account, at least in part, for the large discrepancies associated with the $V_\theta(0)$ predictions discussed above.

A paradox of the Donaldson-Betz method, as applied to flap vortices, is that it predicts a finite centerline peak velocity $V_\theta(0)$, but it precludes direct estimation of r_1, which corresponds to $V_{\theta,max}$ for a real vortex. For the vortices measured in the wake, however, experimental scatter is too large for a meaningful estimate of r_2. Thus, the table shows a comparison of the measured r_1^*/r_1 and the predicted r_2^*/r_2 since these are both a measure of vortex size. Both show an overall decrease in vortex size.

5.2 Outboard Flap – Segmented Actuation

In section 5.1 perturbations were applied over the entire span of the deflected flap. However, if perturbations are introduced locally, along some fraction or segment of the slot, then it is possible that separation can be varied over a finite zone of the flow. This is desirable because then, in principle, the local vortex sheet $\gamma=d\Gamma/dy$ can be varied and hence control can be exerted over a specific vortex, leaving the remainder of the wake unchanged. Simultaneously, lift and moment excursions can be minimized. In the discussion below, the effect of perturbations on the inboard and outboard halves of the flap is considered (cf. section 3 and fig. 2b).
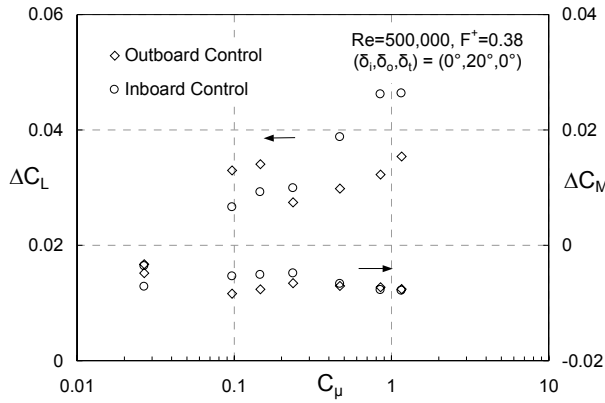
Fig. 9. Lift and moment coefficients for perturbations introduced from the two locations indicated in fig. 2b ($\alpha=8°$).
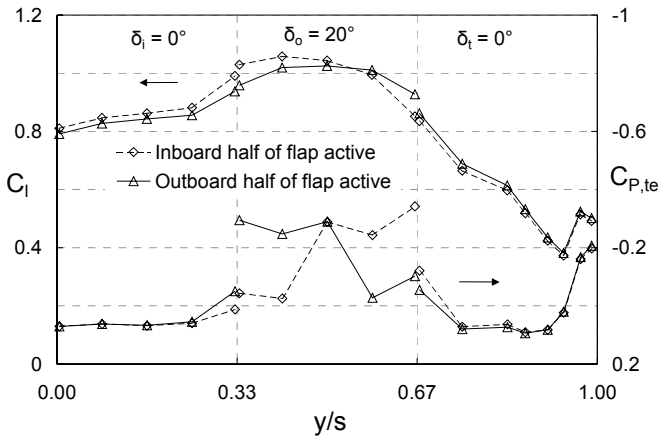
Fig. 10. Trailing-edge pressure recovery and span-loading for perturbations introduced from the two locations indicated in fig. 2b ($\alpha=8°$).

As expected, introducing perturbations from each half of the flap slot resulted in relatively small overall changes to the aerodynamic indicators (fig. 9), namely $\Delta C_L<0.05$ and $\Delta C_M<0.008$ over the full range of control amplitude. These are approximately one third of the excursions observed for full span perturbations (cf. fig. 5 and section 5.1 above). Despite the small changes to the aerodynamic indicators, separation is effectively controlled, as can be seen by the pressure recoveries associated with both inboard and outboard perturbations as well as the significantly different span-loadings (fig. 10). Thus significant control is applied locally to the vortex sheet and this manifests as effective authority over either inboard or outboard vortices.

It is believed that the increase in bound circulation (lift) that accompanies separation control in two-dimensional flows is "lost" to the vortices when control is applied near the flap-edges. Less of this circulation is lost when control is applied remotely from the edges. Thus,

10

control applied near the edges has the potential for significant vortex control accompanied by a negligible effect on the overall aerodynamic forces.

A comparison of wake measurements with rollup relations is shown in tables 2a and 2b. As observed above, superior predictions are associated with changes to the outboard vortex. From the point of view of perturbing the vortex centroid, it is evident that perturbations in the vicinity of the flap-edge result in full control authority ($\Delta \bar{y} / s \geq 2.5\%$), for both the outboard (table 2a) and inboard (table 2b) vortices. It should further be noted that, for almost identical lift, the ratio of inboard to outboard vortex strength (Γ_C' / Γ_B') can be varied from 0.55 (no control) to 0.87 (inboard control only). In fact, the peak inboard vorticity is more than double the outboard peak with inboard perturbations. Varying the strength of a counter-rotating inboard vortex is known to have a profound effect on the wake stability (e.g. Ortega *et al.* [5] and Rennich & Lele [26]).

Table 2a. Effect of segmented separation control on the outboard vortex (B) trailing the midspan flap.

	Inboard Control		Outboard Control	
	7-hole probe	Donaldson-Betz	7-hole probe	Donaldson-Betz
$\Delta \bar{y} / s$ (%)	-0.34	-0.48	-2.50	-2.21
Γ'^* / Γ'	1.03	1.09	1.24	1.05
$V_\theta^*(0) / V_\theta(0)$	0.94	1.17	1.54	1.36
r_1^* / r_1	0.89	—	0.44	—
r_2^* / r_2	—	0.93	—	0.77

Table 2b. Effect of segmented separation control on the inboard vortex (C) trailing the midspan flap.

	Inboard Control		Outboard Control	
	7-hole probe	Donaldson-Betz	7-hole probe	Donaldson-Betz
$\Delta \bar{y} / s$ (%)	2.73	1.38	0.09	-0.38
Γ'^* / Γ'	1.32	1.38	1.01	1.19
$V_\theta^*(0) / V_\theta(0)$	1.25	1.61	0.85	1.18
r_1^* / r_1	0.41	—	0.91	—
r_2^* / r_2	—	0.86	—	1.01

5.3 Tip-Flap Actuation

The effect of deflecting the tip-flap, with and without control, can be seen from fig. 11a, which shows the surface pressure distribution at the tip-flap midspan. The span-loadings and trailing-edge pressures corresponding to the cases indicated in fig. 11a are shown in fig. 11b. Surface pressures with no flap deflections, that correspond to the same wing lift, are also shown for comparative purposes. Similar data were acquired at higher and lower α, as well as at *Re*=500,000. Fig. 11b shows the substantial increase in tip loading due to the flap deflection alone, i.e. without the introduction of perturbations. Furthermore, the flap deflection resulted in a weak inboard counter-rotating vortex (not shown), consistent with the predictions of Donaldson *et al.* [21] discussed in section 4. Note that the span-loading data near the wing-tip cannot be used as input to the rollup relations, due to the partially rolled-up vortex pressure signature near the tip.
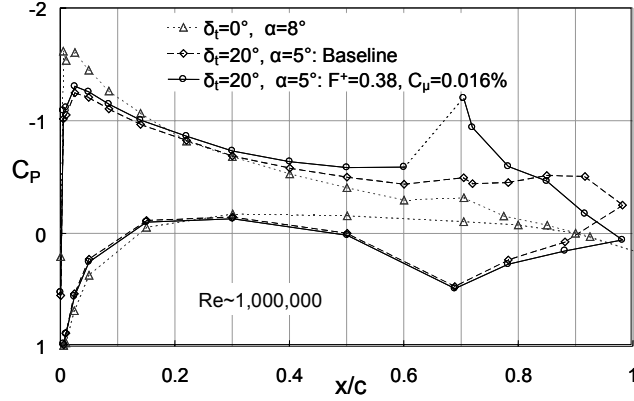
Fig. 11a. Tip-flap center flap pressure distribution at similar wing lift for three cases.
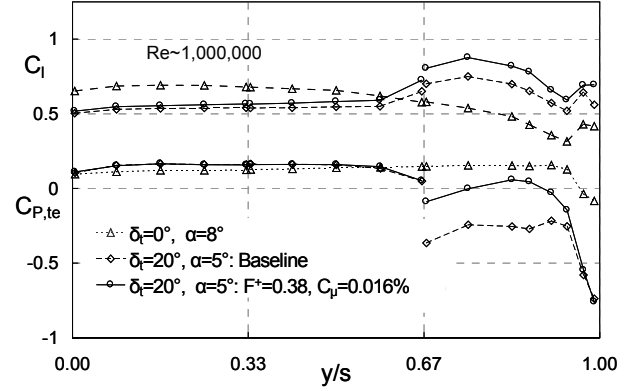
Fig. 11b. Span-loading for the unflapped and flapped configurations, with and without control.

However, a purely theoretical approach could be attempted, along the lines of that by Moore & Saffman [23]. The introduction of perturbations along the entire span of the flap resulted in a mainly local effect as can be seen by the complete pressure recovery on the flap midspan (fig. 11a), while the overall circulation is virtually unaffected. The spanwise extent of the flap pressure recovery and relatively small overall lift enhancement can be seen in fig. 11b. Thus the lift variations that result from control are even smaller than those associated with the midspan flap control, discussed in the previous section. It should be further appreciated that these data represent the largest lift increment attained at F^+=0.38. On this flap, larger C_μ resulted in even smaller excursions (not shown) due to significant non-proportional behavior (cf. fig. 5). It may be concluded that the more three-dimensional the flow, the smaller the changes in the main aerodynamic coefficients, even though separation is significantly manipulated. Furthermore, maximum lift enhancement was attained at particularly small control amplitudes (C_μ=0.016%). This was observed for a range of different Reynolds numbers, angles of attack, as well as control amplitudes and frequencies (not shown). Effective control at low C_μ is highly desirable from an applications perspective due to the practical challenges associated with the introduction of perturbations at flight Reynolds numbers.

Corresponding seven-hole probe measurements of streamwise and in-plane velocity are shown in the wake of the tip flap at x/c=2 for the baseline case (fig. 12a and 12b) and for the controlled case with F^+=0.38 and C_μ=0.016% (fig. 12c and 12d). For the baseline case with no flaps deflected (not shown here), the vortex center is located at around $(y^*/c, z/c) \approx (0.063, 0.003)$. When the flap is deflected with no separation control, the vortex center moves to $(y^*/c, z/c) \approx (0.052, -0.117)$, i.e. a deflection of 1% and 12% of chord inboard and vertically, respectively. The vortex size (both r_1 and r_2) is also larger, and the axial velocity is markedly retarded. It was also observed that the inboard displacement of the tip vortex due to the flap deflection alone at α = 8° was 1% of span, i.e. approximately 2.5 times less than that achieved for the flap vortices subjected to flap-edge perturbations (section 5.1). Furthermore, the cost in terms of lift excursions is seven times smaller. Therefore, exciting vortices by means of separation control should be considered as a viable alternative to the deflection of control surfaces, such as ailerons, to achieve the same purpose.

Introducing control has a dramatic effect on the centerline axial velocity (fig. 12c), where V_{xc}/U_∞ varies from 0.86 to 1.63 for baseline and controlled scenarios respectively (based on

higher resolution measurements near the centerline). This effect is the same as that discussed above with respect to eqn. 11, but the axial velocity difference is much greater for the tip vortex. This is consistent with a much larger peak vorticity in the center of the vortex (cf. figs. 12b and 12d). Despite the large changes to the axial velocity and peak vorticity, the vortex centroid is displaced only 0.25% of the span. This displacement is of the same order as that achieved by varying the angle of attack from 8° to 12° with no flap deflections (not shown). Chevalier [6] demonstrated that pitching a wing in a similar manner resulted in effective excitation of the tip vortices. Here, comparable excitation of the vortex can be achieved with approximately five times less excursion in lift.
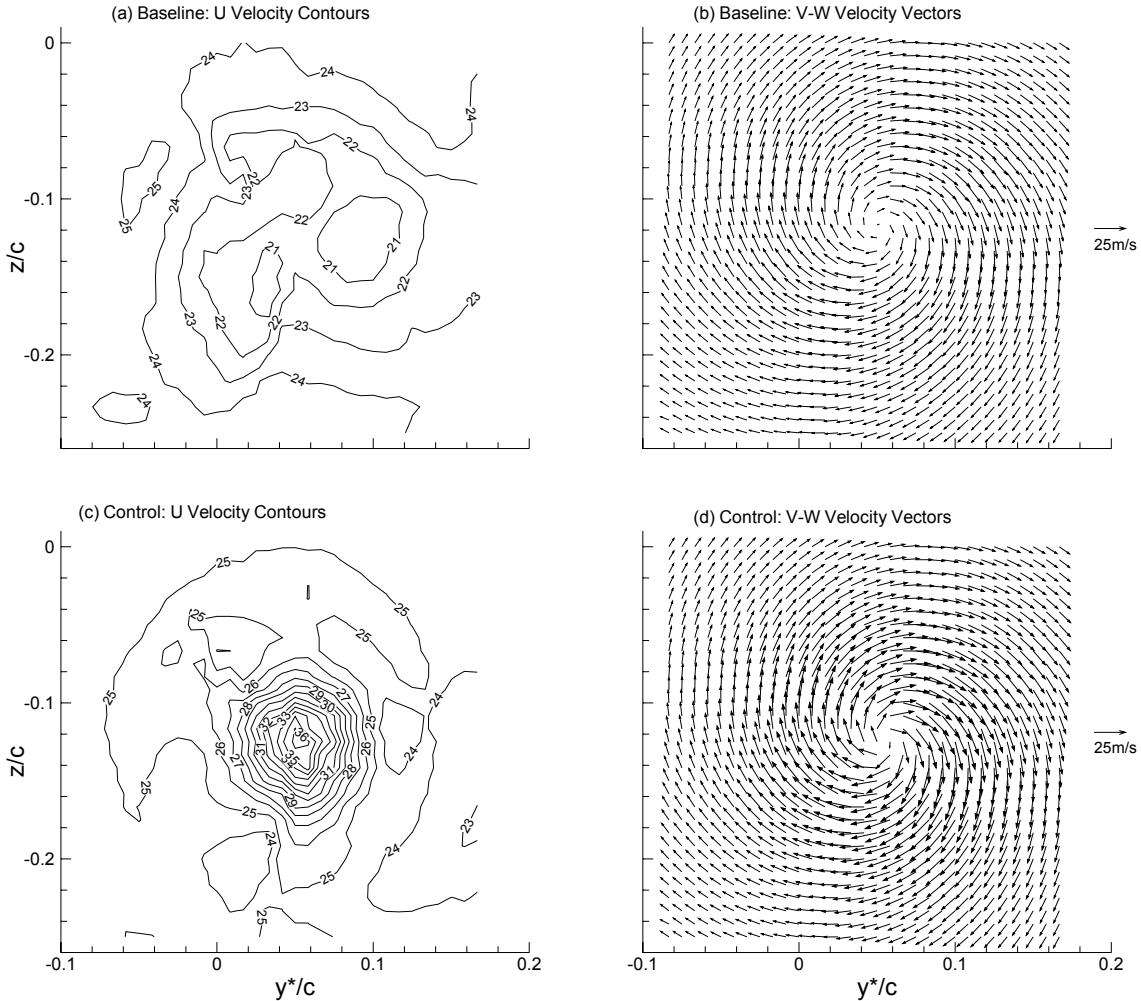
Fig. 12. Seven-hole probe measurements in the wake of the tip flap at x/c=2 for axial velocity (U or V_x) and in-plane velocity vectors (V-W): (a,b) baseline; (c,d) control at F^+=0.38, C_μ=0.016% (α=5°).

6. CONCLUDING REMARKS

Manipulation of the separated flow on a flapped semi-span model had a marked effect on vortex location, strength, tangential velocity, axial velocity and size over a wide range of flap deflections, angles of attack and control conditions. Introduction of perturbations near the flap-edges exerted significant control over either outboard or inboard edge vortices while producing

relatively small lift and moment excursions. In many instances the quantitative vortex characteristics were well predicted by the inviscid rollup relations, which required empirical input in the form of integrated surface pressures.

It is believed that this method will have significant appeal from an industry perspective due to its retrofit potential with no impact on cruise (separation control devices are tucked away in the cove); low operating power requirements (separated flow instabilities are exploited); potentially small lift oscillations when deployed in a dynamic manner; and significant flexibility (application to different high-lift systems or different flight conditions).

REFERENCES

1. Spalart, P. R., "Airplane trailing vortices", *Annual Review of Fluid Mechanics*, Vol. 30, 1998, 107-138.
2. Rossow, V. J., "Lift-generated vortex wakes of subsonic transport aircraft", *Progress in Aerospace Sciences*, Volume 35, Issue 6, 1999, Pages 507-660.
3. Robinson, J. J., "A simulation-based study of the impact of aircraft wake turbulence weight categories on airport capacity," CP-584, AGARD, 1996, pp. 22-1–22-15.
4. Cliffone, D. L. and Orloff, K. L., "Far field wake-vortex characteristics of wings," *AIAA Journal of Aircraft*, Vol. 12, No. 5, 1975, pp. 464-470.
5. Ortega, J. M., Bristol R. L. and Savas, Ö., "Experimental study of the instability of unequal-strength counter-rotating vortex pairs" *J. Fluid Mech.*, Vol. 474, 2003, pp. 35-84.
6. Chevalier H., "Flight test studies of the formation and dissipation of trailing vortices," *Journal of Aircraft*, Vol.10, No. 1, pp. 14-18.
7. Crow, S. C. and Bate E. R., "Lifespan of trailing vortices in a turbulent atmosphere", *Journal of Aircraft*, Vol. 13, No 7, 1976, pp. 476–82.
8. Crouch, J. D., Miller, G. D. and Spalart, P. R., "Active-Control System for Breakup of Airplane Trailing Vortices", *AIAA Journal*, Vol. 39, No. 12, 2001, pp. 2374-2381.
9. Crouch, J. D., "Forcing the breakup of airplane trailing vortices," Conference on Capacity and Wake Vortices, Imperial College of Science, Technology and Medicine, London, England, September 2001.
10. Rudolph, P. K. C., "High-lift systems on commercial subsonic airliners", 1996, NASA CR 4746.
11. van Dam, C. P., "The aerodynamic design of multi-element high-lift systems for transport airplanes", *Progress in Aerospace Sciences*, Volume 38, 2002, pp. 101-144.
12. Bellastrada, C., Breitsamter, C. and Laschka, B, "Investigation of turbulent wake vortex originating from a large transport aircraft in landing configuration", Proc. CEAS Aerospace Aerodynamics Research Conference, 2002, pp 31.1-31.10.
13. Crouch J. D., "Instability and transient growth for two trailing-vortex pairs," *J. Fluid Mech.*, vol. 350, 1997, pp. 311-330.

14. Greenblatt, D. and Wygnanski, I, "Control of separation by periodic excitation", *Progress in Aerospace Sciences*, Volume 37, Issue 7, 2000, pp. 487-545.

15. Leishman, J. G., "Principles of Helicopter Aerodynamics", Cambridge University Press, Cambridge, UK, 2000.

16. McAlister, K. W., Tung, C. and Heineck, J. T., "Devices that alter the tip vortex of a rotor", NASA TM-2001-209625, AFDD TR-01-A-003, 2001.

17. Liu, Z., Sankar L. N., Hassan A. A., "A study of rotor tip vortex structure alteration techniques" *AIAA Journal of Aircraft*, Vol. 38, No. 3, May-June 2001.

18. Dawson, S., Marcolini, M., Booth, E., Straub, F., Hassan, A., Tadghighi, H. and Kelley, H., "Wind Tunnel Test of an Active Flap Rotor: BVI Noise and Vibration Reduction," Proceedings of the 51st Annual Forum of the American Helicopter Society, Fort Worth, Texas, 1995, pp. 631-648.

19. Splettstößer, W. R., Kube, R., Seelhorst, U., Wagner, W., Boutier, A., Michali, F., Merker, E., and Pengel, K., "Key results from a higher harmonic control aeroacoustics rotor test (HART) in the German-Dutch Wind Tunnel", 21st European Rotorcraft Forum, St. Petersburg, Russia, 1995.

20. Jacklin, S. A and Nguyen, K., "Full-scale wind tunnel test of a helicopter individual blade control system", American Helicopter Society 50th National Forum, Washington DC, 1994.

21. Donaldson, C duP., Snedeker, R. S. and Sullivan, R. D., "Calculation of aircraft wake velocity profiles and comparison with experimental measurements", *AIAA Journal of Aircraft*, Vol. 11, No. 9, 1974, pp. 547-555.

22. Donaldson, C duP., "A brief review of the aircraft trailing vortex problem", A.R.A.P. Report No. 155, AFOSR-TR-71-1910, 1971.

23. Moore, D.W. and Saffman, P.G., "Axial flow in laminar trailing vortices," *Proc. R. Soc., London Ser. A* 333, 1973, pp. 491–508.

24. Donaldson, C duP. and Bilanin, A. J., "Vortex wakes of conventional aircraft", AGARDograph No. 204, 1975.

25. Batchelor G.K., "Axial flow in trailing line vortices", *J. Fluid Mech.*, Vol. 20, part 2, 1964, pp. 645–58.

26. Rennich, S. C. and Lele, S. K., "Method for Accelerating the Destruction of Aircraft Wake Vortices," *AIAA Journal of Aircraft*, Vol. 36, No. 2, 1999, pp. 398-404.